Available online at www.sciencedirect.com

ScienceDirect

www.elsevier.com/locate/mod

The p38 MAPK signalling pathway is required for glucose metabolism, lineage specification and embryo survival during mouse preimplantation development

Berna Sozen [a], Saffet Ozturk [a], Aylin Yaba [b], Necdet Demir [a,*]

[a] *Department of Histology and Embryology, Akdeniz University, School of Medicine, Campus, 07070, Antalya, Turkey*

[b] *Department of Histology and Embryology, Istanbul Medipol University, School of Medicine, 34810, Beykoz, Istanbul, Turkey*

Received 27 December 2014; received in revised form 18 May 2015; accepted 19 May 2015
Available online 27 May 2015

Abstract

Preimplantation embryo development is an important and unique period and is strictly controlled. This period includes a series of critical events that are regulated by multiple signal-transduction pathways, all of which are crucial in the establishment of a viable pregnancy. The p38 mitogen-activated protein kinase (MAPK) signalling pathway is one of these pathways, and inhibition of its activity during preimplantation development has a deleterious effect. The molecular mechanisms underlying the deleterious effects of p38 MAPK suppression in early embryo development remain unknown. To investigate of the effect of p38 MAPK inhibition on late preimplantation stages in detail, we cultured 2-cell stage embryos in the presence of SB203580 for 48 h and analysed the 8-cell, morula, and blastocyst stages. We determined that prolonged inhibition of the p38 MAPK altered the expression levels of *Glut1* and *Glut4*, decreased glucose uptake during the 8-cell to blastocyst transition, changed the expression levels of transcripts which will be important to lineage commitment, including *Oct4/Pou5f1*, *Nanog*, *Sox2*, and *Gata6*, and increased cell death in 8-16 cell stage embryos onwards. Strikingly, while the expression levels of *Nanog*, *Gata6* and *Oct4*/*Pou5f1* mRNAs were significantly decreased, *Sox2* mRNA was increased in SB203580-treated blastocysts. Taken together, our results provide important insight into the biological processes controlled by the p38 MAPK pathway and its critical role during preimplantation development.

Keywords: Preimplantation; Mouse; P38 MAPK; GLUT; Lineage segregation

* Corresponding author. Tel.: +90 242 2496884; fax: +90 242 2274486.
E-mail address: necdet08@yahoo.com (N. Demir).

http://dx.doi.org/10.1016/j.mod.2015.05.002
0925-4773/

1. Introduction

Preimplantation development is a conserved process in mammalians and is vital for successful implantation and pregnancy. This period of development is characterised by development of the zygote through consecutive cleavage divisions, activation of embryonic transcription, and morphogenetic events, including compaction and cavitation, that result in the formation of the blastocyst (Duranthon et al., 2008; Fleming et al., 2000; Fujimori, 2010; Watson and Barcroft, 2001). Although glucose is not utilised as an energy source in the early preimplantation embryos in mouse, it becomes the major energy substrate at the time of compaction during which a high energy source is required to facilitate morphogenetic events, including cavitation and blastocyst formation (Gardner and Leese, 1988; Gardner et al., 2000). Embryos have an absolute requirement for glucose to maintain normal proliferative, differentiative and metabolic development (Pantaleon et al., 2008). During the metabolic adaptation process, the facilitative glucose transporter (GLUT; also known as SLC2A) family of proteins provides an adaptation capability of the preimplantation embryo for variable environmental conditions and metabolic requirements (Hogan et al., 1991; Leppens-Luisier et al., 2001; Purcell and Moley, 2009). GLUT isoforms perform distinct functions in maintaining glucose homeostasis within the embryo and allow the developing embryo to increase its glucose uptake in response to growth and proliferative stimuli by the translocation of carriers from intracellular stores to the plasma membrane (Leppens-Luisier et al., 2001; Pantaleon et al., 2008; Purcell and Moley, 2009).

As this metabolic transition occurs, the embryo undergoes a morphological restructuring process known as compaction (hereafter defined as the late stage embryo (Leese, 1995)), specialisation occurs, and three distinct lineages can be distinguished within the developing blastocyst: the pluripotent epiblast (EPI) and two extraembryonic lineages—the trophectoderm (TE) and the primitive endoderm (PE) (Sozen et al., 2014). To commit to a lineage, specific transcriptional networks must be established to reinforce the cell fate decision (Yamanaka et al., 2006; Zernicka-Goetz et al., 2009). These complex processes are regulated by a number of dynamic cell-signalling pathways. Disruption of these processes and the interactions within these pathways can impact the developmental potential and/or the survival of the embryo (Oron and Ivanova, 2012). Therefore, determining the intracellular signalling pathways that regulate early embryogenesis is crucial for understanding the biological requirements for a healthy pregnancy.

Although many of the biological processes, transport systems and transcripts important in regulating cell fate during preimplantation development are well defined, little is known about the intracellular signal mediators that control these molecules and subsequent cell fate decisions. p38 mitogen-activated protein kinase (MAPK), one of the intracellular signal mediators, is ubiquitously expressed in all eukaryotic cells and regulates gene expression, mitosis, migration and apoptosis (Ono and Han, 2000; Pearson et al., 2001). Studies have demonstrated that the entire p38 MAPK pathway is present and plays both developmental and adaptive roles throughout preimplantation development (Bell and Watson, 2013; Natale et al., 2004). The cytokine-suppressive anti-inflammatory drugs (CSAIDs™, pharmacological inhibitors of p38 MAPK) are potent and specific pharmacological agents that are routinely and reliably used to investigate p38 MAPK function in cell systems (Cargnello and Roux, 2011). Several studies using CSAIDs have previously shown that p38 MAPK plays roles in

the regulation of preimplantation development, including its observed roles in the regulation of cavitation and tight junction function (Bell and Watson, 2013; Maekawa et al., 2005). Although p38 MAPK inhibition with CSAID-treatment leads to developmental retardations primarily in late preimplantation stages (Maekawa et al., 2005; Natale et al., 2004), the underlying causes of this effect is mostly unknown. In addition, evidence suggests that p38 MAPK signalling is involved in regulating the expression of GLUT proteins (especially GLUT1 and 4) and mRNAs (Montessuit et al., 2004; Riera et al., 2009; Yamamoto et al., 2000).

These data led us to investigate, in detail, the exact roles of p38 MAPK signalling during preimplantation development. We wished to elucidate the mechanisms underlying the regulation of glucose transporter expression and the potential role of p38 MAPK signalling in lineage segregation. In the present study, 2-cell stage embryos were cultured in the presence of SB203580 (a p38 MAPK pharmacological inhibitor) for 48 h up to the blastocyst stage. Developmental potential, cell death, glucose uptake, glucose transporter expression and cell fate-related gene expression levels were evaluated. We have shown that the GLUT1 and GLUT4 protein expression and glucose uptake were predominantly decreased; *Glut1*, *Glut4*, *Oct4*/*Pou5f1*, *Nanog*, *Sox2*, and *Gata6* mRNA levels were altered; and cell death was induced by prolonged inhibition of p38 MAPK signalling. Based on these results, we suggest that the deleterious effects on early mouse embryos due to inhibition of p38 MAPK activity likely result from the alterations on the glucose transport and incorrect lineage segregation.

2. Material and methods

2.1. Superovulation and embryo collection

Six-week-old BALB/c female and 12-week-old BALB/c male mice were maintained in the Experimental Animal Care and Production Unit of the School of Medicine at Akdeniz University. All protocols performed were approved by the Akdeniz University Institutional Animal Care and Use Committee (protocol no: 2011.09.65). Female mice were superovulated with an intraperitoneal (i.p) injection of 5 IU of PMSG (Sigma-Aldrich), followed 48 h later by 5 IU of hCG (Sigma-Aldrich). Immediately after hCG injection, female mice were mated with 12-week-old BALB/c males, and the mating status was confirmed by the identification of a vaginal plug the following morning (considered as 0.5 dpc). Timing post-hCG was used to predict embryonic development, and two-cell embryos were obtained by puncturing the ampulla portion of the oviduct with a needle in HEPES-buffered media under the stereomicroscope (Zeiss).

2.2. Embryo culture and drug treatment

SB203580, one of the p38 MAPK specific inhibitors, or CSAID™, (Calbiochem) was prepared in dimethyl sulphoxide (DMSO, Sigma-Aldrich) to make a 20 mM stock concentration and was stored at −20 °C until use. All embryo culture procedures were performed in G-1™/G-2™ Plus sequential media (Vitrolife) (Summers and Biggers, 2003). The G-1™ Plus media used for developing cleavage stage embryos (from the 2-cell to

compact 8-cell stage; interval between 0–24 h), and then embryos were transferred to the G-2™ Plus media up to the blastocyst stage (interval between 24–48 h). Two-cell stage embryos were collected, washed, pooled and cultured in three microdrop culture treatments: (1) media alone (control, n = 295), (2) media plus 0.1% DMSO (vehicle-control, n = 295), and (3) media plus 20 μM SB203580 (drug-treated, n = 363). *In vitro* culture for each group was performed in 50 μl culture drops, overlaid with 3 ml of light mineral oil (Sigma-Aldrich) in a 35-mm culture dish (Becton–Dickinson), and all incubations were performed with 5% CO_2 at 37 °C. Control drops without an embryo were included in every dish to control for non-specific changes in glucose concentration in the medium. Two-cell stage embryos (0 h) were cultured up to the 8-cell (24 h), compact morula (36 h) and blastocyst stages (48 h) in each culture treatment. During *in vitro* culture, embryos obtained from each group were assessed and compared for morphology, progression through cleavage divisions, and blastocyst formation rates.

2.3. Quantitative real-time PCR (qRT-PCR)

Quantitative real-time polymerase chain reaction (qRT-PCR) of whole embryos was performed to determine the effects of p38 MAPK inhibition on the mRNA levels of the glucose transporter genes *Glut1* and *Glut4* and the cell fate and pluripotency regulators, *Oct4*/*Pou5f1*, *Nanog*, *Sox2*, and *Gata6*.

2.3.1. RNA extraction and reverse transcription

RNA extraction and reverse transcription protocols were performed as described in our previous study (Ozturk et al., in press). Briefly, a pool of 30 embryos at the appropriate stages from each group were obtained and stored in lysis buffer at −80 °C until use. Total RNA was extracted using the RNAaqueous Microkit (Ambion) according to the manufacturer's instructions. To eliminate DNA contamination, extracted RNA was treated with DNase I (Ambion). The Reverse Transcription (RT) reaction was performed using the RETROscript kit (Ambion) according to the manufacturer's instructions. The samples were incubated with random decamer primers at 85 °C for 3 min to remove any secondary structures and were then incubated with a reverse transcription reaction composed 2 μl of 10× RT buffer, 4 μl of 1.25 mM dNTP mix, 1 μl of RNase inhibitor (10 units/μl) and 1 μl of MMLV-RT (100 units/μl) at 44 °C for 1 h. Finally, the MMLV-RT enzyme was inactivated at 92 °C for 10 min.

2.3.2. PCR amplification

The qRT-PCR reactions were performed on a Rotor-Gene (Corbett Research). Each 25-μl qRT-PCR reaction mixture contained 12.5 μl of 2× SYBR green supermix (Qiagen), 0.4 μM of each primer and 1 μl of cDNA template. The primer pairs used to amplify *beta actin*, *Glut1*, *Glut4*, *Oct4*/*Pou5f1*, *Nanog*, *Sox2*, and *Gata6* are reported in Table 1. *Beta actin* was used as an internal control housekeeping gene to normalise the expression of target genes. PCR amplifications were performed for 45 cycles in which the initial 3 min denaturation was at 95 °C followed by a program consisting of 10 cycles of 92 °C for 20 s, 65 °C for 20 s, and 72 °C for 60 s; and then by 35 cycles of 92 °C for 20 s, 55 °C for 15 s, and 72 °C for 60 s. The relative gene expression levels were calculated by using $2^{-\Delta\Delta Ct}$ (cycle threshold) method. Thus, the relative *Glut1*, *Glut4*, *Oct4*/*Pou5f1*, *Nanog*, *Sox2*, and *Gata6* gene

expression in the embryos obtained from three groups were reported as the fold change. Note that the qRT-PCR reactions were established triplicates, and this experiment was repeated two times. Furthermore, the specificity of *Glut1*, *Glut4*, *Oct4*/*Pou5f1*, *Nanog*, *Sox2*, *Gata6* and *beta actin* qRT-PCR products was confirmed by a melting curve analysis.

2.4. D-Glucose measurement in culture media

A measurement of D-glucose in the culture medium in each group was performed using a glucose (HK) assay kit (Sigma-Aldrich). Briefly, this method is based on an enzymatic analysis of D-glucose by hexokinase and the consequent increase in NADH (Martin and Leese, 1999). NADH reactions are measured spectrophotometrically at 340 nm, and the NADH concentration is directly proportional to the D-glucose concentration in the sample. The control (embryo-free) and spent incubation drops from each experimental group were collected every 24 h and stored at −80 °C until analysis. Calibrated pipettes were used to add samples of medium from the control and spent incubation drops to the reaction mixture. After a 15-minute incubation, the absorbance at 340 nm was measured by spectrophotometer (BioTek). Taking into consideration the compounds in the sequential media, D-glucose standards for each medium sample were separately generated and included in each assay. Then, the D-glucose concentration was calculated in each experimental group and compared. The D-glucose concentration in the control (embryo-free) incubation drops was accepted as 100%, and the percentage of glucose consumption in spent drops among the treatment groups was calculated. All reactions were performed in triplicate.

2.5. Whole-mount indirect immunofluorescence

Embryos were first washed in 1% bovine serum albumin (BSA) in PBS (0.1 M, pH 7.4) and were then fixed in 3% paraformaldehyde (PFA) in PBS for 20 min at room temperature and washed three times in 1% BSA in PBS. The fixed embryos were permeabilised and blocked by incubation for 1 h in 2% BSA in PBS with 0.01% Triton X-100 at room

Table 1Sequence of the primers for the genes used in this study.

Gene	Primer	Primer sequence (5′ → 3′)	Product size (bp)
Glut1	F	TGTGTACTGCGGCCTGACTACTG	399
	R	AACAGCTCCAAGATGGTGACCTTC	
Glut4	F	AAGATGGCCACGGAGAGAG	415
	R	GTGGGTTGTGGCAGTGAGTC	
Oct4/Pou5f	F	CTGTAGGGAGGGCTTCGGGCACTT	485
	R	CTGAGGGCCAGGCAGGAGCACGAG	
Nanog	F	AGGGTCTGCTACTGAGATGCTCTG	364
	R	CAACCACTGGTTTTTCTGCCACCG	
Sox2	F	GGCAGCTACAGCATGATGCAGGAGC	131
	R	CTGGTCATGGAGTTGTACTGCAGG	
Gata6	F	CGAGGAATCAAAAGTCAGG	53
	R	AGTCAAGGCCATCCACTGTC	
β-actin	F	TGCGTGACATCAAAGAGAAG	244
	R	CGGATGTCAACGTCACACTT	

temperature. The embryos were then washed three times in 1% BSA in PBS. The primary antibodies, rabbit anti-GLUT1 (Abcam) (1:200), rabbit anti-GLUT4 (Abcam) (1:100), rabbit anti-phospho-MAPKAP2 (Cell signalling) (1:100), rabbit anti-phospho-HSP27 (cell signalling) (1:50), mouse anti-Cdx2 (BioGenex) (1:200), goat anti-Oct3/4 (Abcam) (1:100), and goat anti-Nanog (RD Systems) (1:100) were diluted in 1% BSA in PBS with 0.01% Tween-20 and incubated at 4 °C overnight. To detect the primary antibody, the embryos were incubated with anti-mouse Alexa Flour-488, anti-goat Alexa Flour-555, anti-rabbit Alexa Flour-488-conjugated secondary antibodies (Invitrogen) diluted 1:350 in 1% BSA in PBS with 0.01% Tween-20 for 1 h at room temperature. To visualise DNA within nuclei, embryos were treated with 1 mg/ml (1:2000) DAPI for 10 min at room temperature. Fully processed embryos were mounted onto glass slides in 10 μl of a glycerol:PBS (1:1) mixture and analysed with fluorescence microscopy (Olympus, Tokyo, Japan).

2.6. Double immunofluorescence for apoptosis assessment

After 48 h in culture treatment, the blastocyst stage embryos in each experimental group were obtained, washed, fixed, permeabilised and blocked as described above. A cocktail of primary antibodies including mouse anti-Cdx2 (BioGenex) (1:200) or goat anti-Oct3/4 (Abcam) (1:100) and rabbit anti-cleaved caspase-3 (Cell Signalling) (1:100) were prepared in 1% BSA in PBS plus 0.01% Tween-20 and incubated at 4 °C overnight. A cocktail of anti-mouse Alexa Flour-488 or anti-goat Alexa Flour-488 and anti-rabbit Alexa Flour-555 conjugated secondary antibodies (Invitrogen) (1:350) were prepared in 1% BSA in PBS with 0.01% Tween-20, and embryos were incubated for 1 h at room temperature. Embryos were washed, nuclear staining was performed, and embryos were mounted as described above.

Both whole-mount indirect and double immunofluorescence staining experiments were applied to three replicates, and 10–15 embryos for control, vehicle control and drug treatment groups were examined for each of the primary antisera. Additionally, negative controls were conducted in which embryos were exposed to the same procedure in the absence of primary antibody to assess the levels of background and non-specific binding of the secondary antibody.

2.7. TUNEL assay

The embryos were fixed in 4% PFA prepared in PBS for 20 min at room temperature, washed three times in PBS, and permeabilised in PBS with 1% sodium citrate and 0.01% Triton X-100 for 15 min at 4 °C. The embryos were then washed three times in PBS. The 10–15 embryos from control, vehicle control, and drug treatment groups were placed in 50 μl of TUNEL reaction mixture (Roche) for 1 h at 37 °C in the dark. The negative control embryos were put into 50 μl of TUNEL label solution (Roche) only. The embryos were then washed 1 mg/ml (1:2000) DAPI for 10 min at room temperature (Sigma-Aldrich). Fully processed embryos were mounted onto glass slides in 10 μl of a glycerol:PBS (1:1) mixture and analysed. Each embryo was analysed for total number of nuclei and number of TUNEL-labelled nuclei. In the present study, the proportion of the TUNEL-positive nuclei to total number of cells was defined as TUNEL-stained nuclei. The TUNEL staining for each group was performed three times.

2.8. Statistical analysis

All results were first subjected to a normality test and once passed, they were analysed by a repeated measure ANOVA test followed by a Holm-Sidak test for qRT-PCR analysis and Dunn's test for TUNEL findings. All error bars represent standard error of the mean (SEM) values. A P value of <0.05 was considered significant. Statistical calculations were performed using SigmaStat for Windows, version 3.5 (Jandel Scientific Corp).

3. Results

3.1. Inhibition of p38 MAPK signal primarily affects late preimplantation

With the inhibition of p38 MAPK activity, the embryos displayed morphological abnormalities, showing a developmental blockade at the 8–16 cell stage onwards ($P < 0.05$) (Fig. 1), consistent with previous studies (Maekawa et al., 2005; Natale et al., 2004; Paliga et al., 2005).

Two-cell stage embryos cultured in the presence of SB203580 progressed to the 8-cell stage (78.12% ± 9.04%) slightly less frequently than the untreated controls (88.69% ± 8.74%) and the DMSO treated group (89.13% ± 9.39%) after 24 h of culture (Fig. 1A). The proportion of the compact morula after 36 h in culture was significantly reduced in the SB203580-treated group (66.78% ± 7.18%) compared with the control (85.85% ± 8.9%) and DMSO-treated (83.13% ± 10.11%) groups ($P < 0.05$) (Fig. 1A). Following 48 h in culture, the frequency of 2-cell embryos developing to the blastocyst stage was dramatically reduced in the SB203580-treated group (43.21% ± 8.42%) compared with the control (81.78% ± 8.72%) and DMSO-treated (77.19% ± 11.15%) groups ($P < 0.05$) (Fig. 1A). The p38 MAPK blockade appears more evident in late preimplantation stages because the most apparent phenotype occurred from the 8–16 cell stages onwards. Additionally, an increase in arrested (25.21% ± 8.79%) and degenerate (30.68% ± 8.79) embryos cultured in the presence of SB203580 were found when compared with the control (9.79% ± 8.75% for arrested embryos, 5.57% ± 7.9% for degenerate embryos) and DMSO-treated (10.0% ± 7.1% for arrest embryo, 6.7 ± 8.7 for degenerate embryo) groups ($P < 0.05$) (Fig. 1A).

Although developmental and morphological abnormalities were not apparent after 24 h in culture (Fig. 1B) in the presence of the inhibitor, differences were observed during the 24–48 h interval of treatment. Most SB203580-treated embryos did not complete compaction (Fig. 1B). Whereas some embryos treated with SB203580 compacted normally, they displayed cavitation failure or formed a much smaller cavity than control embryos (Fig. 1C). Additionally, following 48 h of treatment, blastocysts in the presence of the inhibitor displayed reduced expansion and hatching rates and had a thick zona pellucida structure (Fig. 1C).

3.2. SB203580 treatment affects the expression levels of glucose transporters

To define the underlying mechanisms of developmental blockade at the 8–16 cell stages onwards following p38 MAPK inhibition (Fig. 1A), we investigated the expression levels of glucose transporter proteins and genes because glucose transport is prominent in late

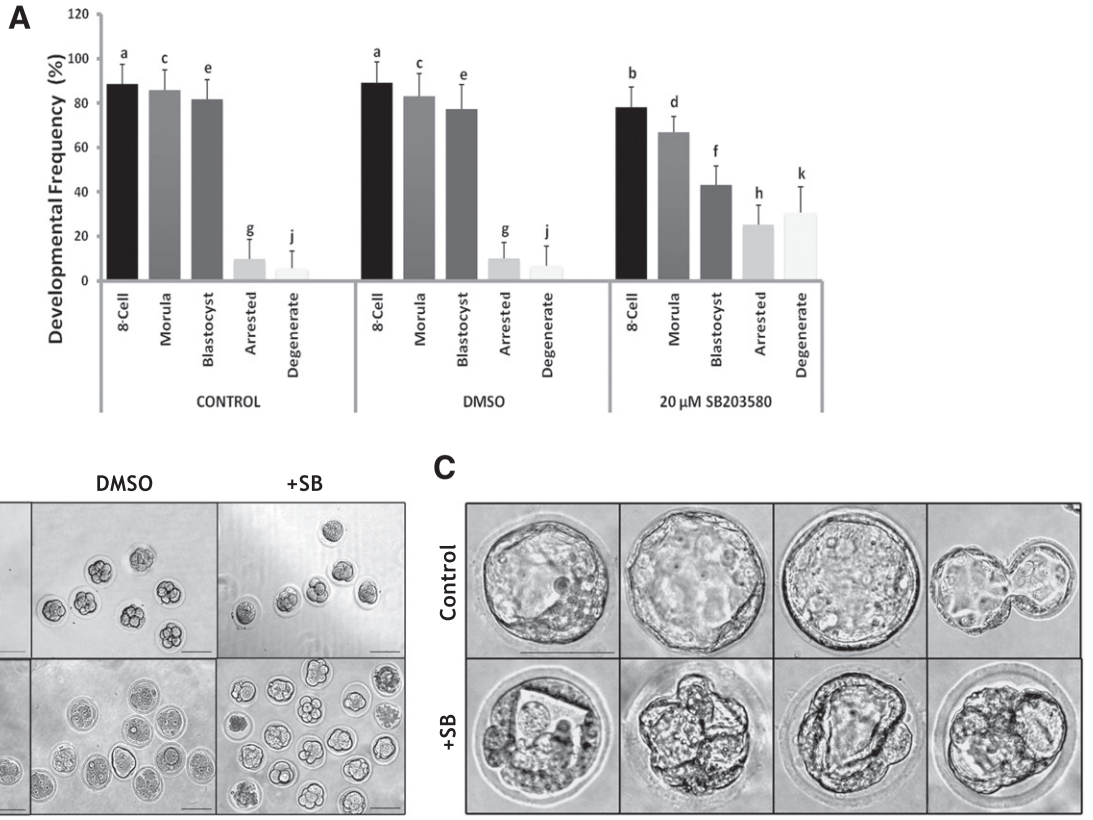
A
Developmental Frequency (%)
120
100
80
60
40
20
0
a
c
e
g
i
a
c
e
g
j
b
d
f
h
k
8-Cell
Morula
Blastocyst
Arrested
Degenerate
CONTROL
DMSO
20 µM SB203580
B
Control
DMSO
+SB
8-Cell
Morula
C
Control
+SB

stage embryos. Firstly, to confirm the effectiveness of the p38 MAPK inhibitor, the protein expression levels of p-MK2 and p-HSP27 (downstream targets of p38 MAPK) were analysed in all treatment groups (Maekawa et al., 2005; Natale et al., 2004; Paliga et al., 2005). Expectedly, all SB203580-treated embryos displayed a complete loss of the expression levels of both proteins (Fig. 2). GLUT1 protein and mRNA levels were analysed in the 8-cell, morula and blastocyst stage embryos. GLUT4 protein and mRNA were analysed only in blastocysts because GLUT4 expression is restricted to the blastocyst stage in embryos (Purcell and Moley, 2009). According to our results, in control groups, GLUT1 protein was normally distributed on the basolateral plasma membrane of the 8-cell and morula stage embryos, and it was found to be expressed in trophectoderm cells and uniformly on the plasma membrane of the inner cell mass in blastocysts (Fig. 3). Following 24 h of culture, GLUT1 protein expression did not change at the 8-cell stage embryos among groups. However, dramatically decreased GLUT1 protein expression was observed in SB203580-treated morula (36 h) and blastocysts (48 h). GLUT4 protein expression was analysed and detected in the cytoplasm and perinuclear area of control and vehicle blastocysts. However, although weak dot-like reactions were detected in the cytoplasm, GLUT4 protein expression was decreased in blastocysts in the presence of the inhibitor (48 h) (Fig. 3).

qRT-PCR analysis revealed that p38 MAPK inhibition altered *Glut1* and *Glut4* mRNA levels. The expression of *Glut1* mRNA levels remained unchanged in 8-cell stage embryos among groups (Fig. 4A). However, in the presence of SB203580, *Glut1* mRNA levels were remarkably decreased ($P = 0.03$) in morulas and were significantly increased in blastocysts ($P < 0.001$) compared with the controls (Fig. 4A). *Glut4* mRNA expression in the blastocysts was predominantly decreased ($P < 0.001$) in the inhibitor group compared with the control groups (Fig. 4B). No significant difference for either gene studied here was observed between the control and vehicle groups (Fig. 4).

3.3. Reduced glucose uptake from culture media in late preimplantation

Because the protein and mRNA expression levels of the glucose transporters were found to be affected in p38 MAPK-inhibited embryos, we next examined spent incubation droplets to detect glucose uptake from their microenvironment. The change of D-glucose

Fig. 1. Developmental frequency from 2-cell stage embryos to blastocyst stages during *in vitro* culture treatments. Two-cell stage mouse embryos were cultured in the absence of inhibitor (control), 0.1% DMSO (vehicle-control) and 20 μM SB203580 (p38 MAPK inhibitor) for 48 h. Eight-cell stage embryos represent 24 h of treatment, the morula stage represents 36 h of treatment, and the blastocyst stage represents 48 h of treatment. (A) In the presence of the inhibitor, the percentage of developing embryos was significantly reduced ($P < 0.05$). Additionally, arrested and degenerate embryo rates increased in the presence of SB203580 ($P < 0.05$). Significant differences among groups are represented with distinct letters; a–b indicate eight-cell embryos, c–d indicate morulas, e–f indicate blastocysts, g–h indicate arrested embryos, and j–k indicate degenerate embryo frequencies. (B) The morphological appearance of early embryos in different culture treatments. The control and vehicle groups progressed normally to 8-cell and morula stages, whereas the p38 MAPK-inhibited embryos predominantly remained uncompacted following 36 h of treatment. Additionally, some of embryos appeared fragmented and lysed. Scale bar represents 50 μm. (C) The morphological appearance of blastocysts. p38 MAPK-inhibited embryos display morphological defects and developmental regression. Scale bar represents 50 μm. The same magnification was used in all images represented here.

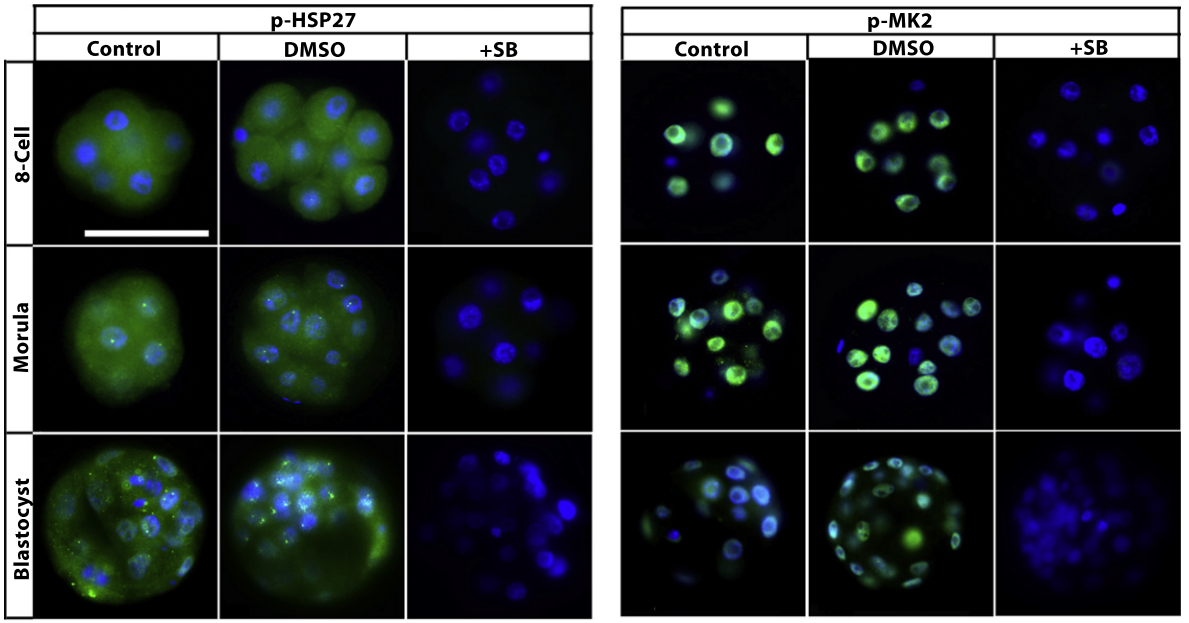

Fig. 2. Phosphorylation of MK2 and HSP27 in the presence of p38 MAPK inhibition. SB203580-treated embryos displayed a complete loss of p-MK2 and p-HSP27 proteins at each developmental stage (N = 27 per groups). The green signal indicates positive staining for the respective primary antibody, and the blue signal (DAPI) indicates nuclei. Scale bar represents 50 μm. The same magnification was used in all images represented here.

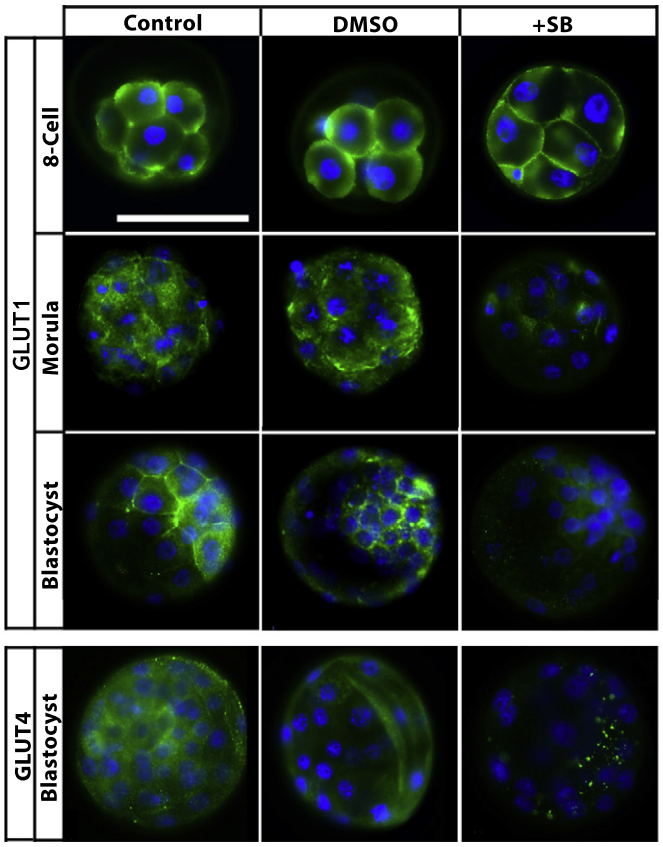

Fig. 3. Effect of p38 MAPK inhibition on GLUT1 and GLUT4 protein expression. Representative images for GLUT1 and GLUT4 in the absence and presence of SB203580. GLUT1 was normally distributed on the plasma membrane of embryonic cells, and GLUT4 was normally distributed in the cytoplasm of embryonic cells as shown in the control groups. GLUT1 expression was not affected by the 8-cell stage (N = 10) but decreased in the morula stages following SB203580 treatment (N = 12). Both proteins' expression levels decreased dramatically in the blastocyst in the presence of the inhibitor (N = 16). The green signal indicates positive staining for the respective primary antibody, and the blue signal (DAPI) indicates nuclei. Scale bar represents 50 μm. The same magnification was used in all images represented here.

concentration in culture medium at 24 and 48 h was assessed using a spectrophotometric glucose measurement assay. Following 24 h of treatment (representing the 2- to 8-cell transition), no significant difference in D-glucose concentration in the culture media was observed among groups (Fig. 5A). However, after 48 h of treatment (representing the 8-cell to blastocyst transition), D-glucose concentration in the culture media of SB203580-treated embryos was significantly higher than in control groups ($P < 0.01$) (Fig. 5A). The D-glucose concentration in the control (embryo-free) incubation drops was normalised to 100%, and the glucose uptake from culture media during the 2- to 8-cell transition was calculated to be 6.16%, 5.34%, and 4.23%; and during the 8-cell to blastocyst transition

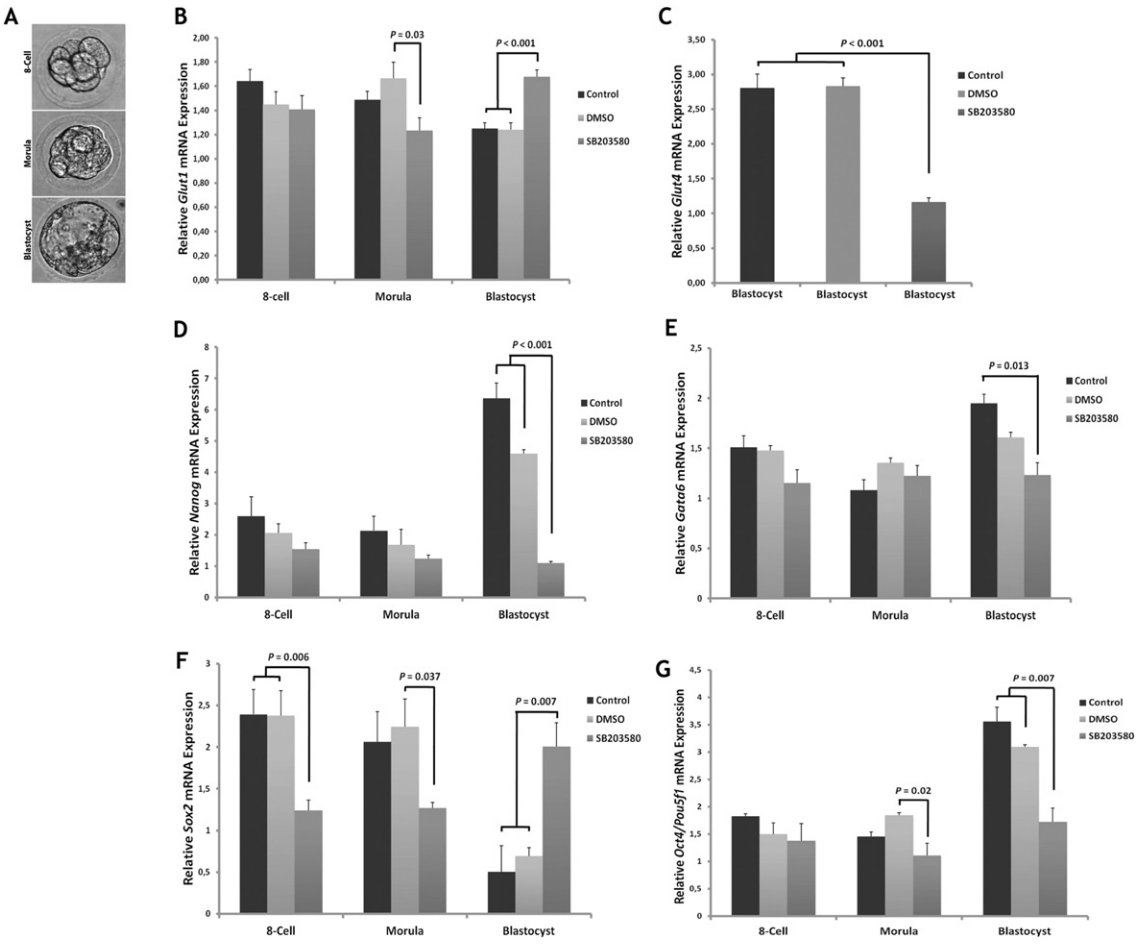
A
8-Cell
Morula
Blastocyst
B
Relative Glut1 mRNA Expression
P = 0.03
P < 0.001
Control
DMSO
SB203580
8-cell
Morula
Blastocyst
C
Relative Glut4 mRNA Expression
P < 0.001
Control
DMSO
SB203580
Blastocyst
Blastocyst
Blastocyst
D
Relative Nanog mRNA Expression
P < 0.001
Control
DMSO
SB203580
8-Cell
Morula
Blastocyst
E
Relative Gata6 mRNA Expression
P = 0.013
Control
DMSO
SB203580
8-Cell
Morula
Blastocyst
F
Relative Sox2 mRNA Expression
P = 0.006
P = 0.037
P = 0.007
Control
DMSO
SB203580
8-Cell
Morula
Blastocyst
G
Relative Oct4/Pou5f1 mRNA Expression
P = 0.007
P = 0.02
Control
DMSO
SB203580
8-Cell
Morula
Blastocyst

was calculated to be 10.42%, 12.77%, and 4.08% in the control, DMSO-treated and drug-treated groups, respectively (Fig. 5B).

3.4. SB203580 treatment affects lineage-specific gene expression

To elucidate the effect of p38 MAPK inhibition on the expression levels of lineage-specific transcription factors, we performed qRT-PCR analysis for the EPI-specific homeobox transcription factor *Nanog*, the PrE-specific factor *Gata6* and the ICM/EPI-specific factors *Oct4*/*Pou5f1* and *Sox2* (Yamanaka et al., 2006).

The expression levels of *Nanog*, *Gata6* and *Oct4*/*Pou5f1* mRNAs were significantly decreased after 48 h of SB203580 treatment in blastocyst stage embryos ($P < 0.05$) (Fig. 4C,D,F). In contrast, the expression level of *Sox2* mRNA decreased at the 8-cell ($P = 0.006$) and morula stages ($P = 0.037$) and then increased at the blastocyst stages ($P = 0.007$) compared with the control groups (Fig. 4E). In order to determine whether these factors were also mis-localised in the SB203580-treated blastocysts, we performed double immunofluorescence analysis for OCT3/4, NANOG and CDX2 proteins. Although no remarkable changes have been observed for OCT3/4 expression, NANOG was misexpressed with a number of CDX2 expressing cells when compared with the control blastocysts (Fig. 6).

3.5. Inhibition of p38 MAPK signalling increases cell death in blastocyst stage embryos

The number of DNA-fragmented nuclei and the total number of cells per embryo were evaluated by TUNEL staining (Fig. 7A,B). In the presence of SB203580, blastocysts contained fewer cells (mean 62 ± 2.35) ($P = 0.023$) (Fig. 7C) and had an increased percentage of TUNEL-positive nuclei (8.25% ± 1.32%) compared with the control (1.11% ± 0.33%) and vehicle groups (1.08% ± 0.34%) ($P < 0.001$) (Fig. 6D).

3.6. Inhibition of p38 MAPK signalling increases apoptosis primarily in the ICM layer

Because increased cell death was found in the blastocysts in the presence of SB203580, we aimed to identify which of the embryonic layers was most affected by the suppression of p38 MAPK signalling activity. Double immunofluorescence staining, using a combination of cleaved caspase-3 as an apoptotic marker and CDX2 as a TE layer marker or OCT3/4 as an ICM marker, was performed in each blastocyst group. A normal distribution and staining intensity of CDX2 were found among all treatment groups. However, an increased cleaved caspase-3 reactivity was observed in the drug-treated blastocysts, as expected (Fig. 8). Additionally, the cleaved caspase-3 signal overlapped with the OCT3/4 signal, whereas it did not overlap with the CDX2 signal, indicating that the expression was found in ICM cells (Fig. 8).

Fig. 4. Effect of p38 MAPK inhibition on the relative expression of the glucose transporters and lineage-specific genes. qRT-PCR of whole embryos was applied to determine A) representative DIC images of the SB203580-treated embryos. B) *Glut1*, C) *Glut4*, D) *Nanog*, E) *Gata6*, F) *Sox2*, and G) *Oct4*/*Pou5f1* mRNA levels in each treatment group ($N = 30$ per groups). Significant differences were observed in mRNA expression among groups for each gene studied. Most significant differences were observed in blastocyst stage embryos ($P < 0.05$).

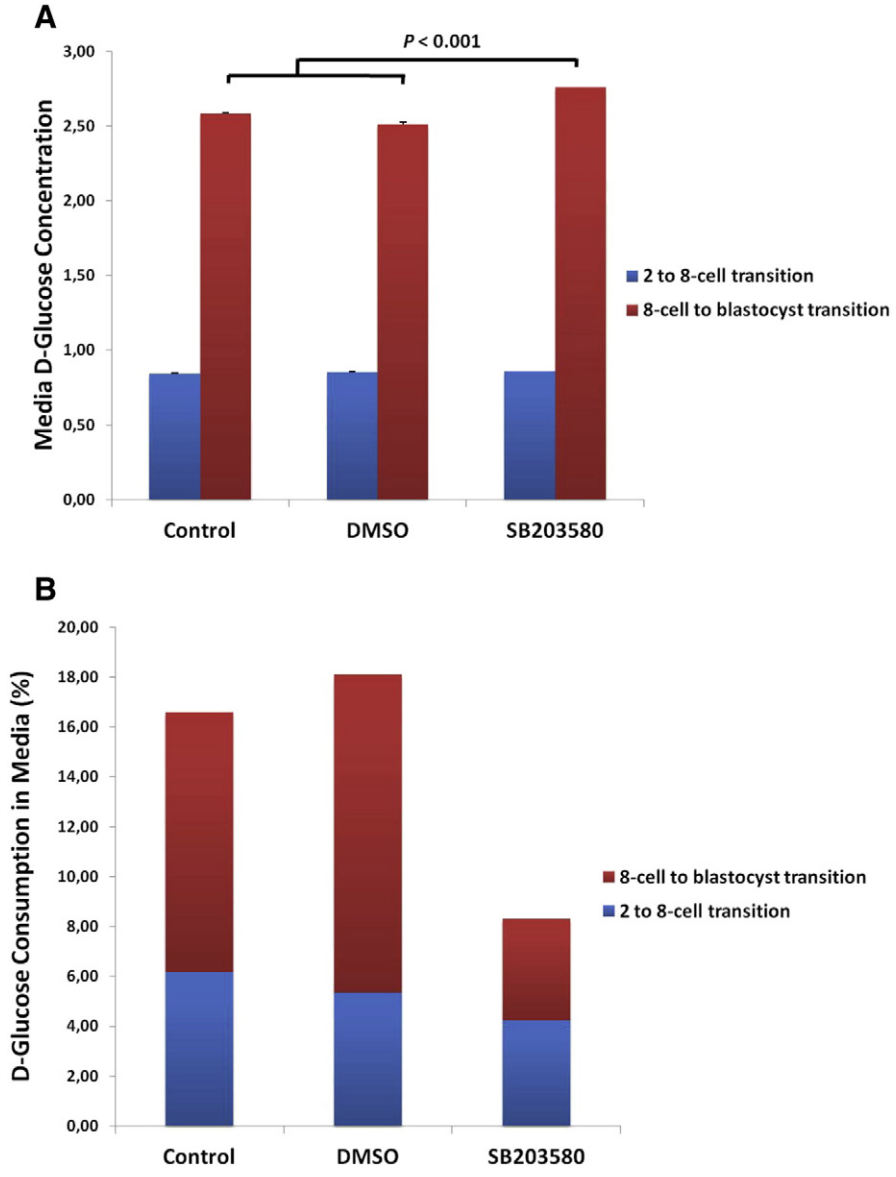

Fig. 5. Inhibition of p38 MAPK affects glucose uptake from media. D-glucose concentrations from spent incubation droplets were measured after 24 h (representing the 2-cell to 8-cell transition, $N = 20$ embryos per groups) and 48 h (representing the 8-cell to blastocyst transition, $N = 20$ embryos per groups) of treatment. A) The D-glucose concentration in the media between treatment groups. After 48 h of treatment, D-glucose concentration was significantly higher than in control groups ($P < 0.01$), indicating no utilisation by embryos. B) The rates of glucose uptake in the culture media among groups.

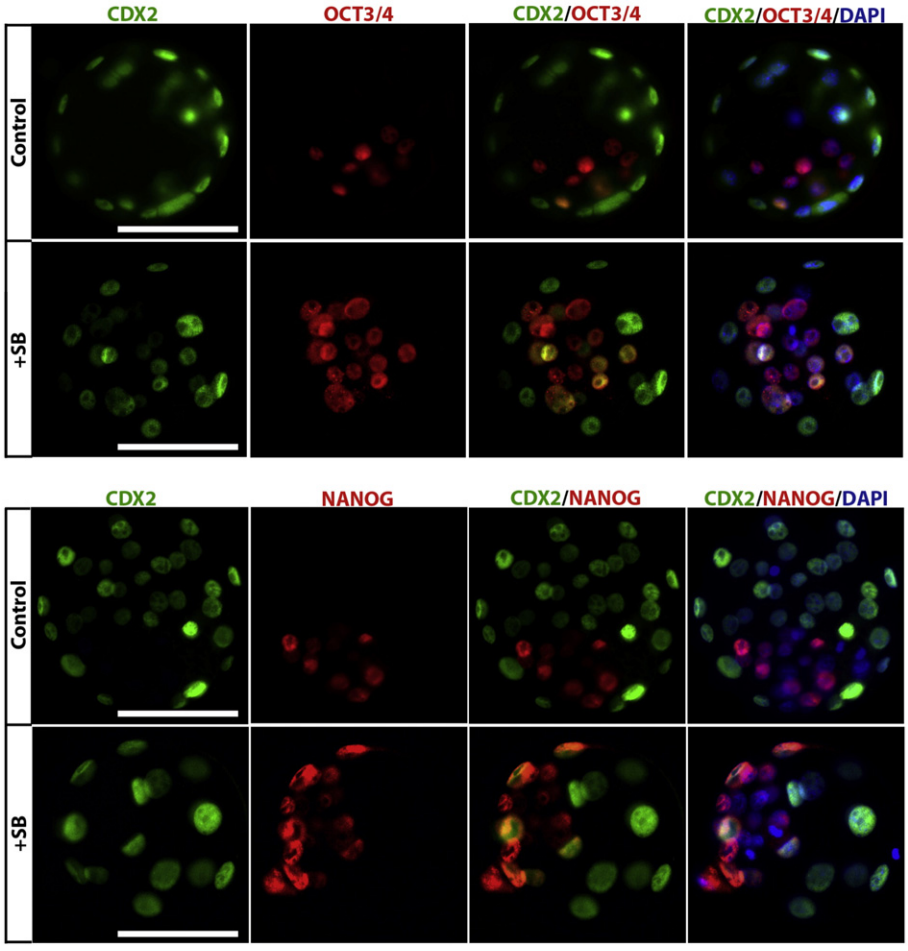

Fig. 6. Effect of p38 MAPK inhibition on lineage-associated protein expressions. Representative images of double-labelled blastocysts after 48 h treatment (N = 3 embryos per group). The green signal indicates positive staining for CDX2, the red signal indicates positive staining for OCT3/4 or NANOG and the blue signal (DAPI) indicates nuclei of the embryonic cells. No remarkable change for the OCT3/4 expression was observed in the SB203580-treated blastocyst when compared with the control blastocysts. On the other hand, NANOG is misexpressed with a number of CDX2 expressing cells and is not similar to the control embryo. Scale bar represents 50 μm.

4. Discussion

During preimplantation development, embryos go through major alterations in their maternal environment, metabolic needs, cell number and degree of lineage segregation (Fleming et al., 2004; Oron and Ivanova, 2012). The variety of GLUTs present in embryos allows them flexibility to adapt to these changes (Leppens-Luisier et al., 2001; Purcell and Moley, 2009). A decrease in glucose uptake after compaction can compromise the developing potential of embryos because glucose uptake and utilisation is vital for embryo survival and

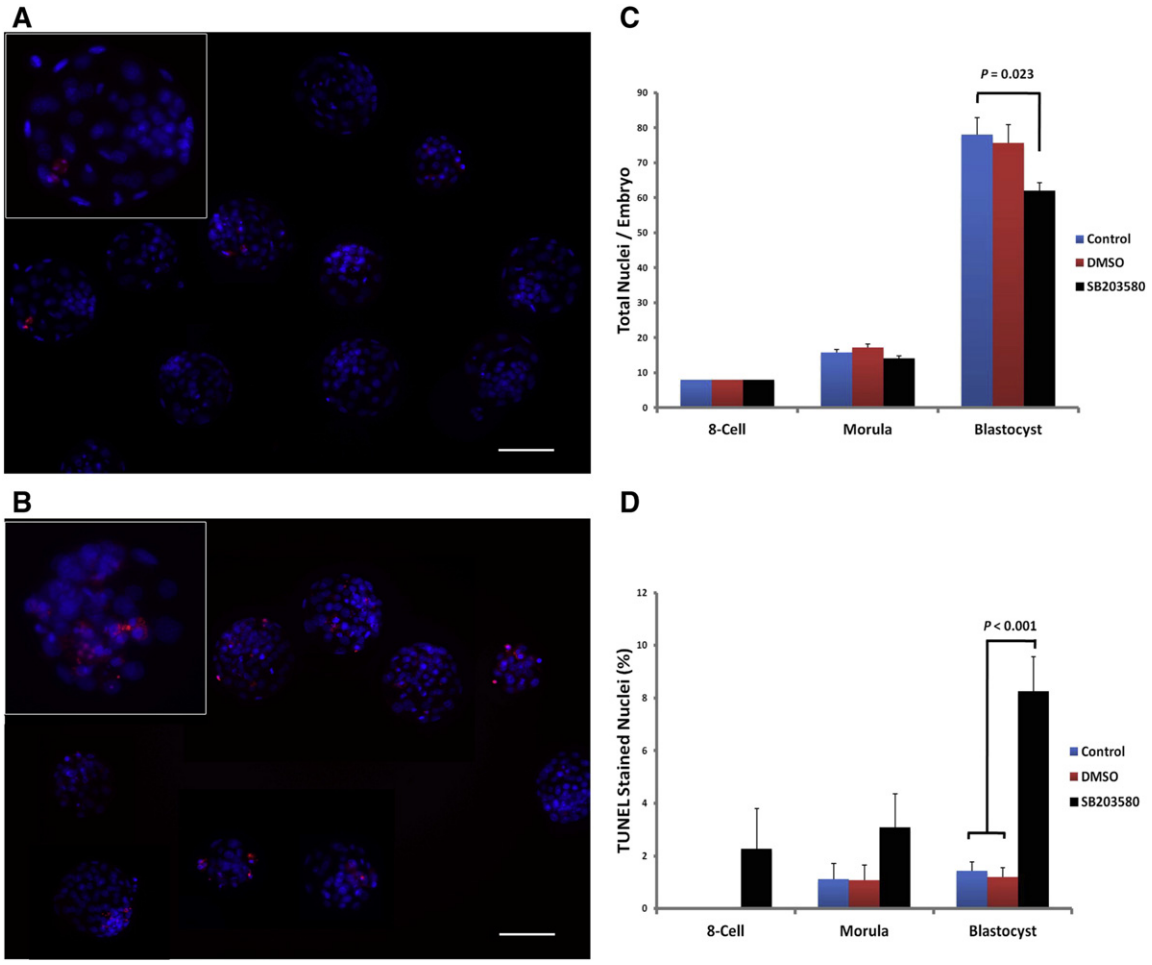
A
B
C
D
P = 0.023
Total Nuclei / Embryo
90
80
70
60
50
40
30
20
10
0
Control
DMSO
SB203580
8-Cell
Morula
Blastocyst
P < 0.001
TUNEL Stained Nuclei (%)
12
10
8
6
4
2
0
Control
DMSO
SB203580
8-Cell
Morula
Blastocyst

development (Riley and Moley, 2006). Thus, defining the intracellular signalling pathways that regulate transporter expression will improve our understanding of the mechanisms involved in reproductive success and failure. In this study, we have investigated p38 MAPK signalling function during development of the preimplantation stage mouse embryo using a specific inhibitor. The results indicate that the p38 MAPK signalling pathway plays a key role in the regulation of GLUT1/GLUT4 protein and mRNA expression and expression levels of transcripts which will be important to lineage commitment. Therefore, altered expression levels of these proteins and genes in the presence of the p38 MAPK blockade seem to be directly related to embryo survival (Fig. 9).

The discovery of a class of compounds called cytokine-suppressive anti-inflammatory drugs (CSAIDs™) allowed us to pharmacologically inhibit p38α (MAPK14) and p38β (MAPK11) isoforms (English and Cobb, 2002). The most extensively characterised CSAIDs are the pyridinyl imidazoles SB203580 (Lee et al., 1994) and SB220025 (Jackson et al., 1998). Numerous studies have used these SB inhibitors in evaluating embryogenesis. Natale et al. (2004) identified p38 MAPK signalling during murine preimplantation development for the first time by using the two different inhibitor molecules, SB220025 and SB203580, in different doses (Natale et al., 2004). The specificity and effectiveness of these inhibitors were demonstrated for each molecule in all doses studied (Natale et al., 2004), and the results revealed that treatment with SB203580 at 20 μM caused the most significant adverse outcomes on embryos (Natale et al., 2004). The same results were also reported by other researchers with the same molecule and dose (Maekawa et al., 2005; Paliga et al., 2005). For this reason, we studied the SB203580 molecule at 20 μM in our study to elucidate the underlying mechanisms in the developmental retardations shown in previous studies. Inhibition of the p38 MAPK signalling pathway was confirmed by decreased expression of its downstream targets, p-MK2 and p-HSP27, as previously shown (Maekawa et al., 2005; Natale et al., 2004; Paliga et al., 2005).

p38 MAPK signalling is important for the preimplantation development period and without this signal activity, embryos display reversible developmental arrest at the 8–16 cell stages onwards (Maekawa et al., 2005; Natale et al., 2004). In the present study, the embryos treated with SB203580 were not morphologically different from control embryos until the onset of compaction. Compaction was inhibited markedly, and those embryos that did compact normally did not cavitate or exhibited a small cavity later on. Our morphological observations are consistent with previous studies (Bell and Watson, 2013; Maekawa et al., 2005; Natale et al., 2004), and the p38 MAPK blockade clearly affects primarily later stage embryos. We next focused on elucidating the underlying mechanism of regression that we observed in late stage preimplantation development. Maekawa et al. (2005) focused on different members of the MAPK signalling pathway and showed that the p38 MAPK and

Fig. 7. Inhibition of p38 MAPK results in increased cell death in the blastocyst. Representative images of TUNEL-labelled blastocysts in A) control (N = 17) and B) drug-treated groups (N = 30), respectively. The red signal indicates TUNEL-positive staining, and the blue signal (DAPI) indicates the nuclei of the embryonic cells. Scale bar represents 50 μm. C) Total number of cells per embryo developed in the treatment groups. p38 MAPK-inhibited blastocysts contained fewer cells (mean 62 ± 2.35, P = 0.023) compared with controls. D) Blastocysts cultured in SB203580 for 48 h displayed a significant increase in the percentage of TUNEL-positive cells (8.25% ± 1.32%, N = 85 ± 2.92 cells, 30 embryos) compared with the controls (1.11% ± 0.33%, N = 19 ± 1.11 cells, 17 embryos) (P < 0.001).

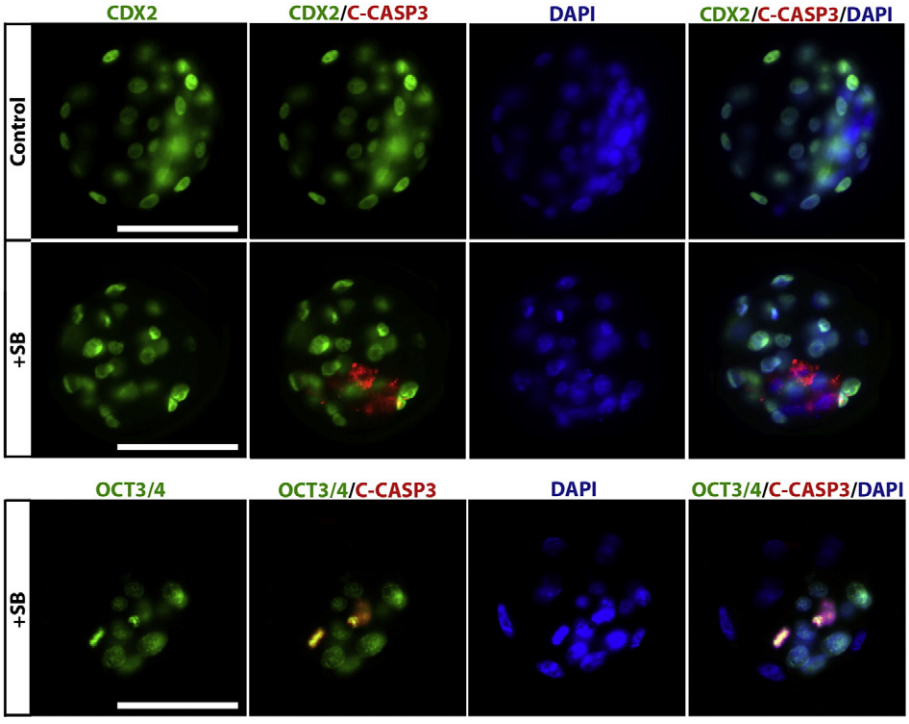

Fig. 8. Increased apoptosis in the ICM layer as a result of p38 MAPK inhibition. Representative images of double-labelled blastocysts after 48 h treatment ($N = 10$ for control, $N = 20$ for drug-treated groups). A) The green signal indicates positive staining for CDX2, the red signal indicates positive staining for cleaved caspase-3, and the blue signal (DAPI) indicates nuclei of the embryonic cells. B) The green signal indicates positive staining for OCT3/4, the red signal indicates positive staining for cleaved caspase-3, and the blue signal (DAPI) indicates nuclei of the embryonic cells. Scale bar represents 50 μm.

JNK pathways are active during mouse preimplantation development and that inhibition of both pathways, but not the ERK pathway, results in an inhibition of cavity formation (Maekawa et al., 2005). A complementary study by Bell and Watson, 2013 (Bell and Watson, 2013) recently demonstrated that suppression of p38 MAPK disrupts cavity formation and tight junction integrity during mouse blastocyst development. With the onset of compaction at the 8-cell stage, embryos require glucose as a high energy source to successfully achieve morphogenetic events, including cavitation and blastocyst formation (Leese and Barton, 1984; Pantaleon et al., 2008). In the absence of glucose, post-compaction development is

Fig. 9. A schematic diagram summarizing the p38 MAPK signalling in the blastocyst stage embryos. As revealed in our findings, the inhibition of p38 MAPK signalling results in decreased expression of GLUT1 and GLUT4 proteins in both TE and ICM cells. In addition, HSP27 and MK2 phosphorylation which dependent of p38 MAPK activity was completely lost in all cells. Our results suggest that the expression levels of *Nanog*, *Gata6* and *Oct4*/*Pou5f1* mRNAs were significantly decreased and Sox2 mRNA were increased in the absence of p38 MAPK signalling in the blastocysts. Following the inhibition of p38 MAPK signalling, decreased glucose uptake, possibly due to altered expression of specific glucose transporters, is also linked to the induction of cell death in embryos, apoptosis primarily in the ICM layer.

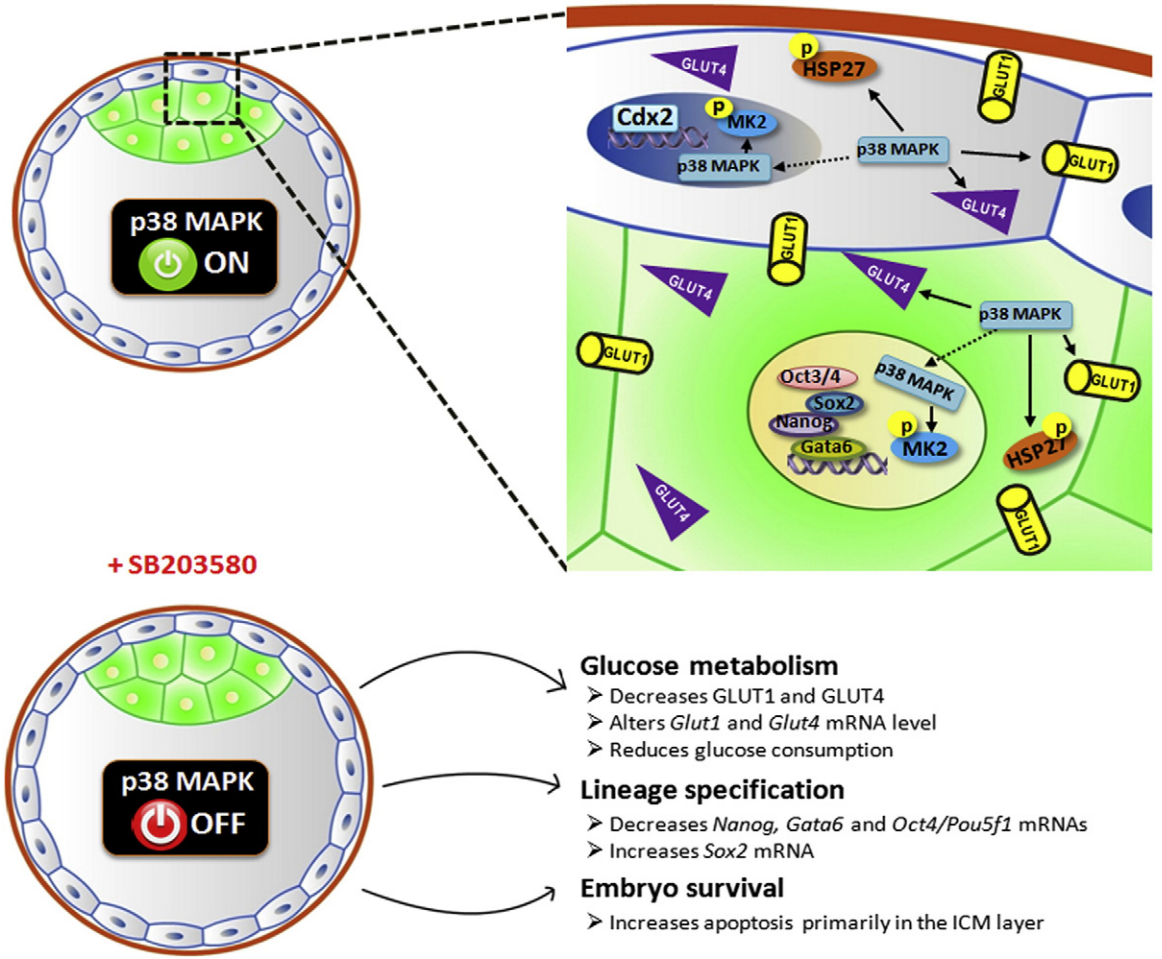
p38 MAPK
ON
GLUT4
p
HSP27
GLUT1
Cdx2
p
MK2
p38 MAPK
p38 MAPK
GLUT1
GLUT4
GLUT1
GLUT4
GLUT4
p38 MAPK
GLUT1
Oct3/4
Sox2
Nanog
Gata6
p38 MAPK
p
MK2
p
HSP27
GLUT1
GLUT4
+SB203580
p38 MAPK
OFF
Glucose metabolism
Decreases GLUT1 and GLUT4
Alters Glut1 and Glut4 mRNA level
Reduces glucose consumption
Lineage specification
Decreases Nanog, Gata6 and Oct4/Pou5f1 mRNAs
Increases Sox2 mRNA
Embryo survival
Increases apoptosis primarily in the ICM layer

inhibited (Pantaleon et al., 2008). We observed that in the absence of p38 MAPK signalling, although GLUT1 protein expression did not change at the 8-cell stage, normal distribution of this protein was disrupted, and its staining intensity was significantly decreased in the morula and blastocyst stage embryos. Further, inhibition of p38 MAPK resulted in a significantly decreased staining intensity of GLUT4 protein in blastocysts. The altered mRNA expression of *Glut1* and *Glut4* were observed in the morula and blastocyst stages. Additionally, when we measured the D-glucose concentration in the culture media, no alteration was observed during the 2- to 8-cell transition, but the D-glucose concentration in the SB-treated group during the 8-cell to blastocyst transition was found to be significantly higher than in the control groups, indicating that SB-treated embryos consumed smaller amounts. Reduced glucose consumption during the 8-cell to blastocyst transition was consistent with altered glucose transporter expressions during late stage embryos following suppression of p38 MAPK. We believe that as a result of glucose transporter protein and mRNA down-regulation, post-compaction embryos have lower intraembryonic glucose concentrations, thereby resulting in developmental failure. As a result of prolonged exposure to the p38 MAPK inhibitor, abnormal blastocyst formation and a reduction in embryo quality may be caused by lower rates of net glucose uptake. Following the inhibition of p38 MAPK signalling, decreased glucose uptake, possibly due to altered expression of specific glucose transporters, is also linked to the induction of cell death in embryos. Taken together, our results demonstrated altered GLUT1/GLUT4 expression in the presence of p38 MAPK inhibition, which is potentially responsible for cavitation and blastocyst formation failures as observed in the present and previous studies.

The p38 MAPK signalling pathway is involved in the regulation of development throughout embryogenesis and primarily acts through regulating gene expression (Calder et al., 2011; Zohn et al., 2006). Calder et al., 2011 investigated the *Glut1* mRNA regulation by MAPK pathways and gas atmosphere and showed that p38 MAPK inhibition with SB220025 for 18 h at the blastocyst stage resulted in a significant reduction of *Glut1* mRNA (Calder et al., 2011). However, although we observed reduced *Glut1* mRNA levels after 24 h and 36 h of treatment, *Glut1* was increased significantly at the blastocyst stage following 48 h of treatment with SB203580. These results suggest that the duration of p38 MAPK inhibition is accompanied by different responses of mRNA production. Additionally, although Calder et al., 2011 suggested that there were no effects of oxygen tension on *Glut1* mRNA (Calder et al., 2011), Kind et al. (2005) demonstrated that culture of mouse embryos under 2% oxygen increased the expression of Glut-1 mRNA when compared to embryos cultured under 7 or 20% oxygen and when compared to *in vivo* developed embryos (Kind et al., 2005). We therefore preferred conventionally used conditions (5% CO_2 in air). In the present study, because embryo culture was performed under the same conditions, we did not expect any expressional changes according to the oxygen pressure between groups.

HSP27, one of the downstream targets of p38 MAPK, participates in the regulation of cell apoptosis by many important apoptotic pathways, as a kind of chaperone protein (Parcellier et al., 2003). Liu et al. (2013) showed that the cell apoptosis in the mouse blastocysts derived from Hsp27 down-regulated zygotes was not significantly changed, and Hsp27 did not affect on early embryo development as a single factor (Liu et al., 2013). In the current study, we demonstrated that the rate of cell apoptosis was significantly increased in the p38 MAPK signalling inhibited blastocysts. As it is known, apoptosis is a complex process involving a number of synergistic genes and proteins, which may play a

compensatory role for abnormal expression of HSP27 during the complex progress of embryonic development. In the absence of p38 MAPK signalling that may be interesting to investigate the other apoptosis-related factors such as the BCL2 family and/or other glucose transporters such as Glut3, which would be helpful to further understand the phenotype of SB203580-treated embryos.

Upon the completion of compaction, asymmetric divisions occur in successive waves, and the cells of the developing blastocyst possess very striking features that identify the precursor cells. After this initial segregation, asymmetrically distributed transcriptional regulators in these precursor cells amplify and transform the gene expression circuitries, and precursors become fully committed. For commitment to occur, the proper specific transcriptional networks must be established to reinforce the cell fate decision. Once TE and ICM precursors are separated, transcription factors, including *Cdx2*, *Tead4* and *Eomes*, are upregulated in outer cells (TE precursors) to enable epithelial specification (Nishioka et al., 2008; Sozen et al., 2014; Strumpf et al., 2005). In contrast, inner cells develop a stable regulatory circuit that includes the transcription factors *Oct4*, *Sox2*, *Gata6* and *Nanog* to promote pluripotency and resist differentiation (Avilion et al., 2003; Mitsui et al., 2003; Nichols et al., 1998). Signalling involving the MAPK isoforms ERK2 and Ras–MapK have been shown to perform specific functions in normal TE development by promoting TE integrity in mouse preimplantation embryos (Lu et al., 2008; Saba-El-Leil et al., 2003). Alternatively, Bell and Watson (2013) recently showed that p38 MAPK inhibition has no impact on CDX2 localisation, suggesting that TE differentiation is well established and is likely unaffected by p38 MAPK inhibition (Bell and Watson, 2013). Consistent with Bell and Watson (2013), we did not observe any changes in CDX2 expression in the presence of the p38 MAPK inhibitor. However, our study demonstrated that *Oct4*/*Pou5f1*, *Nanog*, *Sox2*, and *Gata6* mRNA levels were affected by p38 MAPK inhibition. Furthermore, according to our immunofluorescence results, at 48 h in culture treatment while the control blastocyts had a high NANOG expression restricted to a cluster of cells within the ICM, NANOG is not restricted to the ICM and a number of CDX2 expressing cells on the outside strongly expressed NANOG in SB203580-treated blastocysts. However, studies have previously shown that the NANOG displayed the coexistence with the CDX2 within the same nucleus at early stages and gradually becomes confined to epiblast progenitor cells locating the inside (Chen et al., 2009; Dietrich and Hiiragi, 2007). Having regard to the developmental retardation after SB203580 treatment shown in the present and previous studies, SB203580-treated blastocysts in the present study might lag behind the control blastocysts in the timing of the patterning phases that eventually lead to CDX2/NANOG restricted expression. On the other hand, that misexpression of Nanog at both mRNA and protein levels after SB treatment also suggests that the p38 MAPK pathway is involved in the regulation of this transcription factor. Interestingly, while *Nanog*, *Gata6* and *Oct4*/*Pou5f1* mRNAs were significantly decreased after 48 h of SB203580 treatment in blastocyst stage embryos, *Sox2* mRNA was decreased at the 8-cell and morula stages and then increased at the blastocyst stages compared with the control groups. Sox2 displayed an opposite outcome when compared to the other markers. It is surprising and suggests that the disruption on the balance of the transcriptional dynamic of Sox2–Oct4–Nanog regulatory complex, which is a fundamental regulator maintaining undifferentiated ES cell and epiblast fate (Avilion et al., 2003; Chew et al., 2005). An observed increase in cleaved

caspase-3 staining intensity in ICM cells indicated elevated apoptosis in the ICM layer following p38 MAPK inhibition. These outcomes suggested that different MAPK isoforms may play different roles in lineage segregation during preimplantation. Overall, our results indicate that p38 MAPK signalling blockage leads to a disruption in ICM differentiation and pluripotency maintenance.

We propose that after the prolonged inhibition of p38 MAPK signalling, altered expression of glucose transporter proteins and mRNAs results in inadequate glucose consumption in the microenvironment of the embryo. Subsequent changes in mRNA levels of genes associated with lineage differentiation in the blastocyst may then induce cell death. Overall, our findings provide further insights on the developmental and adaptive roles of p38 MAPK signalling during preimplantation development in the mouse. Future studies aim to assess the further roles of this pathway during preimplantation development.

Acknowledgements

This study was carried out as a part of MSc thesis of Berna Sozen and supported by the Akdeniz University Scientific Research Fund (Project No: 2011.02.0122.005) and the Scientific and Technological Research Council of Turkey (TUBITAK; Grant No. 113S160). The authors thank Suray Pehlivanoglu (PhD) for his kind help in spectrophotometric measurements. Additionally, the authors are grateful to Andy Cox (PhD) for helpful comments and corrections on this article.

References

Avilion, A.A., Nicolis, S.K., Pevny, L.H., Perez, L., Vivian, N., Lovell-Badge, R., 2003. Multipotent cell lineages in early mouse development depend on SOX2 function. Genes Dev. 17, 126–140.

Bell, C.E., Watson, A.J., 2013. p38 MAPK regulates cavitation and tight junction function in the mouse blastocyst. PLoS One 8, e59528.

Calder, M.D., Watson, P.H., Watson, A.J., 2011. Culture medium, gas atmosphere and MAPK inhibition affect regulation of RNA-binding protein targets during mouse preimplantation development. Reproduction 142, 689–698.

Cargnello, M., Roux, P.P., 2011. Activation and function of the MAPKs and their substrates, the MAPK-activated protein kinases. Microbiol. Mol. Biol. Rev. 75, 50–83.

Chen, L., Yabuuchi, A., Eminli, S., Takeuchi, A., Lu, C.W., Hochedlinger, K., Daley, G.Q., 2009. Cross-regulation of the Nanog and Cdx2 promoters. Cell Res. 19, 1052–1061.

Chew, J.L., Loh, Y.H., Zhang, W., Chen, X., Tam, W.L., Yeap, L.S., Li, P., Ang, Y.S., Lim, B., Robson, P., Ng, H.H., 2005. Reciprocal transcriptional regulation of Pou5f1 and Sox2 via the Oct4/Sox2 complex in embryonic stem cells. Mol. Cell. Biol. 25, 6031–6046.

Dietrich, J.E., Hiiragi, T., 2007. Stochastic patterning in the mouse pre-implantation embryo. Development 134, 4219–4231.

Duranthon, V., Watson, A.J., Lonergan, P., 2008. Preimplantation embryo programming: transcription, epigenetics, and culture environment. Reproduction 135, 141–150.

English, J.M., Cobb, M.H., 2002. Pharmacological inhibitors of MAPK pathways. Trends Pharmacol. Sci. 23, 40–45.

Fleming, T.P., Ghassemifar, M.R., Sheth, B., 2000. Junctional complexes in the early mammalian embryo. Semin. Reprod. Med. 18, 185–193.

Fleming, T.P., Kwong, W.Y., Porter, R., Ursell, E., Fesenko, I., Wilkins, A., Miller, D.J., Watkins, A.J., Eckert, J.J., 2004. The embryo and its future. Biol. Reprod. 71, 1046–1054.

Fujimori, T., 2010. Preimplantation development of mouse: a view from cellular behavior. Develop. Growth Differ. 52, 253–262.
Gardner, D.K., Leese, H.J., 1988. The role of glucose and pyruvate transport in regulating nutrient utilization by preimplantation mouse embryos. Development 104, 423–429.
Gardner, D.K., Pool, T.B., Lane, M., 2000. Embryo nutrition and energy metabolism and its relationship to embryo growth, differentiation, and viability. Semin. Reprod. Med. 18, 205–218.
Hogan, A., Heyner, S., Charron, M.J., Copeland, N.G., Gilbert, D.J., Jenkins, N.A., Thorens, B., Schultz, G.A., 1991. Glucose transporter gene expression in early mouse embryos. Development 113, 363–372.
Jackson, J.R., Bolognese, B., Hillegass, L., Kassis, S., Adams, J., Griswold, D.E., Winkler, J.D., 1998. Pharmacological effects of SB 220025, a selective inhibitor of P38 mitogen-activated protein kinase, in angiogenesis and chronic inflammatory disease models. J. Pharmacol. Exp. Ther. 284, 687–692.
Kind, K.L., Collett, R.A., Harvey, A.J., Thompson, J.G., 2005. Oxygen-regulated expression of GLUT-1, GLUT-3, and VEGF in the mouse blastocyst. Mol. Reprod. Dev. 70, 37–44.
Lee, J.C., Laydon, J.T., McDonnell, P.C., Gallagher, T.F., Kumar, S., Green, D., McNulty, D., Blumenthal, M.J., Heys, J.R., Landvatter, S.W., et al., 1994. A protein kinase involved in the regulation of inflammatory cytokine biosynthesis. Nature 372, 739–746.
Leese, H.J., 1995. Metabolic control during preimplantation mammalian development. Hum. Reprod. Update 1, 63–72.
Leese, H.J., Barton, A.M., 1984. Pyruvate and glucose uptake by mouse ova and preimplantation embryos. J. Reprod. Fertil. 72, 9–13.
Leppens-Luisier, G., Urner, F., Sakkas, D., 2001. Facilitated glucose transporters play a crucial role throughout mouse preimplantation embryo development. Hum. Reprod. 16, 1229–1236.
Liu, S., Dai, X., Cai, L., Ma, X., Liu, J., Jiang, S., Cui, Y., 2013. Effect of Hsp27 on early embryonic development in the mouse. Reprod. Biomed. Online 26, 491–499.
Lu, C.W., Yabuuchi, A., Chen, L., Viswanathan, S., Kim, K., Daley, G.Q., 2008. Ras-MAPK signaling promotes trophectoderm formation from embryonic stem cells and mouse embryos. Nat. Genet. 40, 921–926.
Maekawa, M., Yamamoto, T., Tanoue, T., Yuasa, Y., Chisaka, O., Nishida, E., 2005. Requirement of the MAP kinase signaling pathways for mouse preimplantation development. Development 132, 1773–1783.
Martin, K.L., Leese, H.J., 1999. Role of developmental factors in the switch from pyruvate to glucose as the major exogenous energy substrate in the preimplantation mouse embryo. Reprod. Fertil. Dev. 11, 425–433.
Mitsui, K., Tokuzawa, Y., Itoh, H., Segawa, K., Murakami, M., Takahashi, K., Maruyama, M., Maeda, M., Yamanaka, S., 2003. The homeoprotein Nanog is required for maintenance of pluripotency in mouse epiblast and ES cells. Cell 113, 631–642.
Montessuit, C., Rosenblatt-Velin, N., Papageorgiou, I., Campos, L., Pellieux, C., Palma, T., Lerch, R., 2004. Regulation of glucose transporter expression in cardiac myocytes: p38 MAPK is a strong inducer of GLUT4. Cardiovasc. Res. 64, 94–104.
Natale, D.R., Paliga, A.J., Beier, F., D'Souza, S.J., Watson, A.J., 2004. p38 MAPK signaling during murine preimplantation development. Dev. Biol. 268, 76–88.
Nichols, J., Zevnik, B., Anastassiadis, K., Niwa, H., Klewe-Nebenius, D., Chambers, I., Scholer, H., Smith, A., 1998. Formation of pluripotent stem cells in the mammalian embryo depends on the POU transcription factor Oct4. Cell 95, 379–391.
Nishioka, N., Yamamoto, S., Kiyonari, H., Sato, H., Sawada, A., Ota, M., Nakao, K., Sasaki, H., 2008. Tead4 is required for specification of trophectoderm in pre-implantation mouse embryos. Mech. Dev. 125, 270–283.
Ono, K., Han, J., 2000. The p38 signal transduction pathway: activation and function. Cell. Signal. 12, 1–13.
Oron, E., Ivanova, N., 2012. Cell fate regulation in early mammalian development. Phys. Biol. 9, 045002.
Ozturk, S., Yaba-Ucar, A., Sozen, B., Mutlu, D., Demir, N., 2014. Superovulation alters embryonic poly(A)-binding protein (Epab) and poly(A)-binding protein, cytoplasmic 1 (Pabpc1) gene expression in mouse oocytes and early embryos. Reprod. Fertil. Dev. http://dx.doi.org/10.1071/RD14106 (in press).
Paliga, A.J., Natale, D.R., Watson, A.J., 2005. p38 mitogen-activated protein kinase (MAPK) first regulates filamentous actin at the 8-16-cell stage during preimplantation development. Biol. Cell. 97, 629–640.
Pantaleon, M., Scott, J., Kaye, P.L., 2008. Nutrient sensing by the early mouse embryo: hexosamine biosynthesis and glucose signaling during preimplantation development. Biol. Reprod. 78, 595–600.
Parcellier, A., Gurbuxani, S., Schmitt, E., Solary, E., Garrido, C., 2003. Heat shock proteins, cellular chaperones that modulate mitochondrial cell death pathways. Biochem. Biophys. Res. Commun. 304, 505–512.

Pearson, G., Robinson, F., Beers Gibson, T., Xu, B.E., Karandikar, M., Berman, K., Cobb, M.H., 2001. Mitogen-activated protein (MAP) kinase pathways: regulation and physiological functions. Endocr. Rev. 22, 153–183.

Purcell, S.H., Moley, K.H., 2009. Glucose transporters in gametes and preimplantation embryos. Trends Endocrinol. Metab. 20, 483–489.

Riera, M.F., Galardo, M.N., Pellizzari, E.H., Meroni, S.B., Cigorraga, S.B., 2009. Molecular mechanisms involved in Sertoli cell adaptation to glucose deprivation. Am. J. Physiol. Endocrinol. Metab. 297, E907–E914.

Riley, J.K., Moley, K.H., 2006. Glucose utilization and the PI3-K pathway: mechanisms for cell survival in preimplantation embryos. Reproduction 131, 823–835.

Saba-El-Leil, M.K., Vella, F.D., Vernay, B., Voisin, L., Chen, L., Labrecque, N., Ang, S.L., Meloche, S., 2003. An essential function of the mitogen-activated protein kinase Erk2 in mouse trophoblast development. EMBO Rep. 4, 964–968.

Sozen, B., Can, A., Demir, N., 2014. Cell fate regulation during preimplantation development: a view of adhesion-linked molecular interactions. Dev. Biol. 395, 73–83.

Strumpf, D., Mao, C.A., Yamanaka, Y., Ralston, A., Chawengsaksophak, K., Beck, F., Rossant, J., 2005. Cdx2 is required for correct cell fate specification and differentiation of trophectoderm in the mouse blastocyst. Development 132, 2093–2102.

Summers, M.C., Biggers, J.D., 2003. Chemically defined media and the culture of mammalian preimplantation embryos: historical perspective and current issues. Hum. Reprod. Update 9, 557–582.

Watson, A.J., Barcroft, L.C., 2001. Regulation of blastocyst formation. Front. Biosci. 6, D708–D730.

Yamamoto, Y., Yoshimasa, Y., Koh, M., Suga, J., Masuzaki, H., Ogawa, Y., Hosoda, K., Nishimura, H., Watanabe, Y., Inoue, G., Nakao, K., 2000. Constitutively active mitogen-activated protein kinase kinase increases GLUT1 expression and recruits both GLUT1 and GLUT4 at the cell surface in 3T3-L1 adipocytes. Diabetes 49, 332–339.

Yamanaka, Y., Ralston, A., Stephenson, R.O., Rossant, J., 2006. Cell and molecular regulation of the mouse blastocyst. Dev. Dyn. 235, 2301–2314.

Zernicka-Goetz, M., Morris, S.A., Bruce, A.W., 2009. Making a firm decision: multifaceted regulation of cell fate in the early mouse embryo. Nat. Rev. Genet. 10, 467–477.

Zohn, I.E., Li, Y., Skolnik, E.Y., Anderson, K.V., Han, J., Niswander, L., 2006. p38 and a p38-interacting protein are critical for downregulation of E-cadherin during mouse gastrulation. Cell 125, 957–969.